

Characterization of a microfocused circularly polarized x-ray probe

J. Pollmann,^{a)} G. Srajer, J. Maser, J. C. Lang, C. S. Nelson, and C. T. Venkataraman
Advanced Photon Source, Argonne National Laboratory, Argonne, Illinois 60439

E. D. Isaacs
Bell Laboratories, Lucent Technologies, Murray Hill, New Jersey 07974

(Received 10 December 1999; accepted for publication 11 February 2000)

We report on the development of a circularly polarized x-ray microprobe in the intermediate energy range from 5 to 10 keV. In this experiment linearly polarized synchrotron radiation was circularly polarized by means of a Bragg-diffracting diamond phase retarder and subsequently focused down to a spot size of about $4 \times 2 \mu\text{m}^2$ by a Fresnel zone plate. The properties of the microprobe were characterized, and the technique was applied to the two-dimensional mapping of magnetic domains in HoFe_2 . © 2000 American Institute of Physics. [S0034-6748(00)01206-5]

I. INTRODUCTION

The magnetic contribution to the cross section for scattering of x rays by matter has been of significant scientific interest for a long time because of its capability to reveal information about the angular and spin momentum distribution in the scattering medium.¹ Since the magnetic contribution is typically several orders of magnitude smaller than the charge contribution, experimentally an intense x-ray beam of well-defined polarization is highly desirable. Only recently, with the advent of high-intensity synchrotron radiation x-ray sources, has it become possible to use polarized x-ray beams, particularly circularly polarized beams, of reasonable intensity to probe magnetic properties of matter, especially of ferromagnets. Furthermore, the availability of high-brilliance synchrotron sources, such as the Advanced Photon Source, the European Synchrotron Radiation Facility, and the Super Photon Ring-8, and of high-quality focusing x-ray optics, such as Fresnel zone plates, has allowed materials characterization on micron and submicron length scales.

In this article, we report the results of combining microfocusing x-ray optics with Bragg-diffracting phase retarders for producing a circularly polarized x-ray microprobe in the energy range from 5 to 10 keV. Such an x-ray beam will enable a wide variety of spatially resolved magnetic scattering experiments, yielding results in applied fields like modern magnetic materials and superconducting compounds, as well as in more basic physics. An important advantage of x rays of this energy is their relatively high penetration power, allowing real bulk measurements of magnetic samples, compared to surface-sensitive techniques like magnetic force microscopy or the magneto-optical Kerr effect. This is especially useful for samples with nonmagnetic surface layers. Compared to neutron scattering, x rays are at an advantage when used to probe for element-specific properties by working at an x-ray resonance.

The requirements for an experiment that uses a microfocused circularly polarized x-ray probe are: (i) the beam incident onto the polarizing optics should be monochromatic and

have a low divergence in order to reach a high degree of polarization after transmission through the phase retarder, (ii) the beam should have good spatial coherence to achieve diffraction-limited resolution with a microfocusing zone plate, and (iii) the x-ray radiation source should deliver an intense beam to yield reasonable count rates (on the order of 10^8 to 10^9 photons per second) after polarizing and focusing optics.

In the following section, we will briefly review the technique for producing a circularly polarized x-ray beam using phase-retarding optics. In Sec. III we will describe the principle of microfocusing with Fresnel zone plates. The experimental setup combining the two optics is described and characterizing results are presented in Sec. IV. In Sec. V, preliminary results on the mapping of magnetic domains in a HoFe_2 crystal are shown. This demonstrates one of the possible applications of the microprobe. Finally, conclusions are given and future improvements of the setup are presented.

II. PHASE-RETARDING OPTICS

Circularly polarized radiation is of particular interest for magnetic x-ray scattering, since it couples linearly to the direction of the magnetic moment, thereby providing sensitivity to the direction of the local moment upon helicity reversal. Several approaches exist for producing circularly polarized x-ray beams from a linearly polarized synchrotron beam.² For the energy range between 5 and 10 keV, however, Bragg transmission phase retarders have proven to be the most practical. The feasibility of using this type of phase retarder was first demonstrated by Hirano and co-workers.³ They utilized the fact that, according to the dynamical theory of x-ray diffraction, the wave fields inside a crystal belonging to different linear directions of polarization propagate with different phase velocities close to a Bragg reflection. The difference in velocities is a function of the deviation $\Delta\theta$ of the angle of incidence from the exact Bragg condition. The phase difference δ thus induced by a crystal of thickness t is given by⁴

^{a)}Electronic mail: pollmann@aps.anl.gov

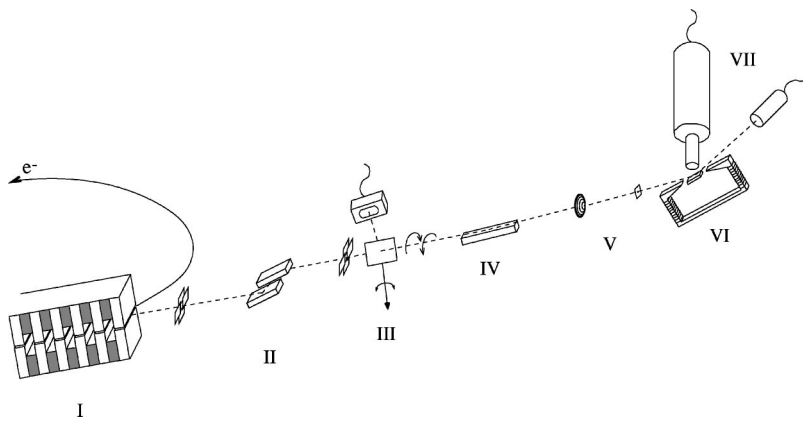


FIG. 1. The experimental setup at the APS beamline 1-ID. The beam coming from the undulator (I) is monochromatized by a double-crystal monochromator (II) and then circularly polarized by a Bragg-transmission diamond phase plate (III). The ion chamber close to the diamond is used to find the diamond (111) Bragg reflection. A Pd mirror (IV) suppresses higher harmonics in the beam. The microfocusing setup (V) consists of the Fresnel zone plate and an order sorting aperture. A magnetic field can be applied to the sample (VI) in the diffraction plane. Different detectors (VII) allow fluorescence as well as diffraction experiments.

$$\delta = \frac{\pi}{2} \left(\frac{r_e \lambda^2}{\pi V} \right)^2 \frac{t \sin(2\theta_B)}{\lambda \Delta \theta \sin(\theta_B)} \Re(F_H F_{\bar{H}}), \quad (1)$$

where r_e is the classical electron radius, λ is the x-ray wavelength, and F_H is the structure factor of the Bragg reflection with Bragg angle θ_B . To obtain circularly polarized radiation with linearly polarized radiation incident on the phase retarder, the phase difference must be $\pi/2$. For arbitrary choice of the thickness of the crystal and the energy of the incident radiation, such a $\pi/2$ phase difference can always be achieved by proper adjustment of the deviation $\Delta\theta$. The degree of polarization of the transmitted x ray is proportional to $\sin(\delta)$ and depends, of course, also on the intensities of the transmitted linear wave fields. Due to their low absorption, diamond crystals are well suited for this application,⁵ with only a few different crystal thicknesses required to cover the whole energy range between 3 and 12 keV.

Since δ is linear in $\Delta\theta$, the transition from one side of the rocking curve of the Bragg reflection to the other ($\pm\Delta\theta$) leads to an inversion of the helicity of circular polarization of the transmitted beam. This rotation of the phase retarder is of the order of tens of arcseconds. Therefore switching the beam helicity requires only minimal time and can be done several times during the course of a measurement, thereby reducing systematic errors. Thus a highly tunable and rapidly switching circular polarizer for x rays can be built.

III. MICROFOCUSING OPTICS

Microzone plates are a well-established tool to produce x-ray beams with submicron cross-section that are used in a variety of different experiments (for a review of recent experiments see Ref. 6). They can be understood as circular diffractive gratings with radially increasing line density, whose operation principle is based on Fresnel's theory of diffracting zones.⁷ By choosing a grating thickness that leads to a phase shift close to $\pi/2$, relatively efficient focusing phase zone plates can be built. Zone plates made of absorbing as well as of phase shifting materials are in use.

The theory of Fresnel zone plates is well understood. The focal length f_m for the m th order of diffraction of a zone plate depends solely on the radius of the innermost zone r_1 and the wavelength of the radiation λ ⁸:

$$f_m = \frac{r_1^2}{m\lambda}. \quad (2)$$

On the other hand, the spatial resolution Δ of a zone plate (i.e., the smallest distance between two points that can be resolved) is a function of the numerical aperture. Using the Rayleigh criterion for Δ and the well-known relations for Fresnel zones, the resolution can be determined from the width of the outermost ring dr_n :

$$\Delta = 1.22 \times \frac{dr_n}{m}. \quad (3)$$

Since the efficiency of a zone plate is proportional to m^{-2} , use of higher diffraction orders for focusing leads to a significant reduction of the efficiency of the zone plate. Several approaches have been proposed to increase the efficiency of Fresnel zone plates, including using high aspect ratios and special zone profiles.⁸

Challenges in the production of zone plates, especially for high-energy x-ray applications, are to achieve a small zone width (and thus a good resolution) and a thickness of the zone plate material that results in the necessary absorption or phase shift at high x-ray energies. Zone plates are manufactured by a combination of electron-beam writing into photoresists and several steps to transfer this pattern to the selected zone plate material. Newer methods use multilayer deposition techniques.⁸

Since the different diffraction orders of a zone plate correspond to distinct focal lengths, an experimental microfocusing setup normally includes an order sorting aperture (OSA), e.g., a pinhole, to reduce unwanted diffraction orders. The position of the OSA between the zone plate and the focus is chosen in such a way that unwanted orders are suppressed due to their divergences, which are different from the divergence of the desired diffraction order.

IV. EXPERIMENTAL SETUP

The polarized microprobe was setup at the 1-ID insertion device beamline at the Advanced Photon Source (APS). Figure 1 shows the setup schematically. The beam was collimated using white-beam tungsten slits close to the source. The radiation was then monochromatized using a standard LN₂-cooled double-crystal Si (111) monochromator. To maximize the flux, the undulator gap was adjusted to the selected energy. An additional set of slits downstream of the

monochromator was used to further define the beam to a size of $0.5 \times 0.5 \text{ mm}^2$ (horizontally \times vertically) 60 m from the source.

This beam was incident on the phase-retarding optics, which was the first component of the polarized microprobe. A $400\text{-}\mu\text{m}$ -thick diamond in (111) reflection geometry was chosen as the phase retarder. This diamond thickness provides a suitable compromise between beam attenuation and a large offset value $\Delta\theta$. A large offset value is desirable, since it minimizes phase-shift variations caused by the divergence and energy spread of the incident beam. For the Ho L-III edge (8.07 keV), the incident flux on the diamond was measured to be $\approx 2 \times 10^{12}$ photons per second, and the transmitted circularly polarized flux was 4×10^{11} photons per second. Although we did not measure the degree of circular polarization in this experiment, it is reasonable to assume a value of 0.99 for the degree of polarization, based on earlier measurements on a similar Bragg transmission phase retarder and calculations using the dynamical theory of x-ray diffraction. In the previous experiments,⁴ we had used a multibeam diffraction method⁹ to determine the Stokes parameters and found excellent agreement with the theory. Furthermore, our estimate of 0.99 is supported by measurements of the degree of circular polarization transmitted through a diamond phase retarder performed by other groups.^{10,11} To suppress higher harmonics, the beam was reflected by a Pd mirror placed after the phase retarder. The beam path was enclosed in evacuated beam pipes to reduce intensity loss due to air scattering.

The microfocusing setup following the diamond consisted of two parts, the zone plate and the OSA. The Au-based zone plate had a thickness of $1.5 \text{ }\mu\text{m}$, a diameter of $250 \text{ }\mu\text{m}$, and a focal length of about 40 cm at 8 keV. It was produced by combined electron-beam and x-ray lithography techniques. The zone plate was mounted on a three-axis motorized stage to allow for linear alignment relative to the sample. Pinholes of various sizes from 20 to $50 \text{ }\mu\text{m}$ were used as OSAs. The OSA mount was motorized for alignment in the x and y directions. The z position (in-beam direction) could be adjusted manually, which was sufficient due to the large focal length of the zone plate.

The alignment of the zone plate, OSA, and center of the standard diffractometer (where the sample was placed) with respect to each other and the x-ray beam was done using a combination of optical and x-ray alignment techniques. First, a transverse prealignment (perpendicular to the beam) was done, watching an image of the x-ray beam on a CdWO_4 scintillator with an optical microscope downstream of the optical components. In this way, diffractometer center, zone plate, and OSA were each subsequently centered on the beam.

Next, the focus of the microfocusing optics had to be positioned on the center of the diffractometer. This was done by placing a Cr-coated knife edge on the diffractometer center. The zone plate and OSA were aligned to the knife edge using the signal of the Cr K-fluorescence. This was done for two perpendicular orientations of the knife-edge to ensure the two-dimensional alignment of the microfocusing setup.

In the next part of the experiment, the size of the micro-

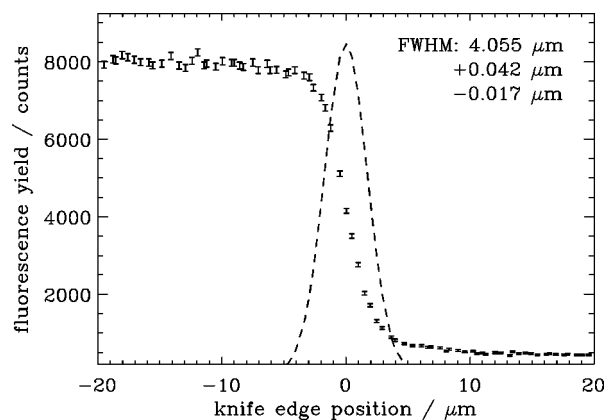


FIG. 2. Horizontal knife-edge scan. Points with error bars represent the measured K-fluorescence yield from the Cr-coated knife edge. The dashed line shows the Gaussian fit to the derivative of the fluorescence signal. The full width at half maximum of this fit is a measure of the size of the focus.

focused beam was measured. This was done by scanning the knife edge, which was mounted on a precision three-axis motorized linear stage with an absolute accuracy better than $0.5 \text{ }\mu\text{m}$ and a relative accuracy of $\approx 10^{-4}$, horizontally and vertically through the beam, and measuring the Cr K-fluorescence of the knife edge as a function of its position. The width of the slope of the fluorescence count rate is a measure of the size of the beam. Quantitative results were obtained from Gaussian fits to the derivative of the signal. Figure 2 shows such a horizontal knife-edge scan together with the obtained Gaussian fit.

Generally, the size of the beam cross-section thus measured is a function of the distance from the focusing zone plate. To find the optimum position for the zone plate, knife edge scans were performed for different distances between the zone plate and the knife-edge. However, the measured spot size for the used zone plate depended only weakly on the distance. This is a consequence of the large focal length of this zone plate, leading to a relatively large depth of focus (of about 1.6 mm). The optimum focus size that could be reached with this zone plate was $4.0 \times 2.3 \text{ }\mu\text{m}^2$ (horizontally \times vertically), with a measured flux on the order of 10^8 photons per second.

Horizontally, the measured focus size agrees very well with the calculated value, taking into account the demagnified size of the source and the divergence of the beam. The vertical size, however, is significantly larger than the calculated value. By temporary clamping the knife edge holder to the zone-plate mounting, it could be shown that this difference is mainly due to vibrations of the knife-edge relative to the zone plate. Other sources of error are imperfections (like slope errors and surface roughness) in the optical components in the beam (monochromator, mirror), which diffract and reflect the beam in vertical direction and thus may introduce distortions.

The knife edge was then replaced by the sample. Three linear motorized stages on the diffractometer offered sufficient degrees of freedom to scan the sample in fluorescence as well as in diffraction geometry. A magnetic field of about 0.2 T could be applied to the sample parallel to the beam.

The experimental setup included two different kinds of

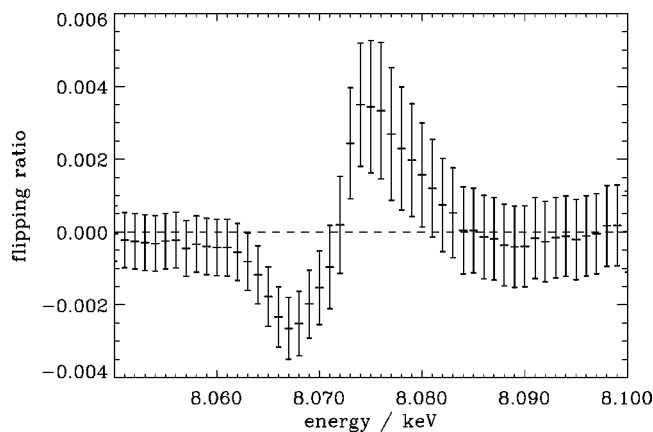


FIG. 3. Measured flipping ratio as a function of energy at the L-III edge of Ho. The maximum normalized difference between the observed transmitted signal for left- and right-circularly polarized incident radiation was less than 1%.

detectors to monitor both the fluorescence yield and the Bragg-scattered intensity as a function of the position of the sample. Since the beam was circularly polarized, there was no preferred direction for the suppression of elastic scattering in the fluorescence detector. A vertical mounting was chosen simply to avoid interference with the sample mounting stage and the electromagnet. Two types of fluorescence detectors can be used in the setup, either a thermoelectric-cooled Cd-Zn-Te detector with 2.2% to 3% energy resolution or a liquid-nitrogen-cooled Si detector with slightly better energy resolution. A Na-I detector mounted on the 2θ arm of the diffractometer placed after collimating slits was used to measure the intensity of the Bragg-diffracted beam.

V. IMAGING MAGNETIC DOMAINS IN HOFe₂

As a demonstration experiment, we used the microprobe to image magnetic domains in a HoFe₂ crystal at the Ho L-III edge. Due to the spin polarization of the 5d orbitals, the magnetic signal for rare earth elements is greatly enhanced close to the L-absorption edges. The difference in the scattering cross-section between left- and right-circularly polarized incident beams can be obtained from the relations given in Ref. 1. Taking into account simplifications which are valid for the geometry of our experiment, it can be written as

$$\Delta\left(\frac{d\sigma}{d\Omega}\right) \approx A(E) \times [m_x \cos(\theta) + m_z \sin(\theta)] \times [1 + \cos(2\theta)], \quad (4)$$

where $A(E)$ comprises the energy dependence of the cross-section and m_x, m_z are the in-plane components of the local magnetic moment. In a first step, $A(E)$ was maximized by doing energy scans with left- and right-circularly polarized radiation and observing the flipping ratio, which is defined as $(I^+ - I^-)/(I^+ + I^-)$, the ratio of the difference of the measured intensities for different polarization directions to the sum of these intensities. To reduce systematic errors arising from a temporal drift in the setup or the synchrotron beam, the intensities for both helicities were measured quasimultaneously by tilting the diamond phase retarder with a fre-

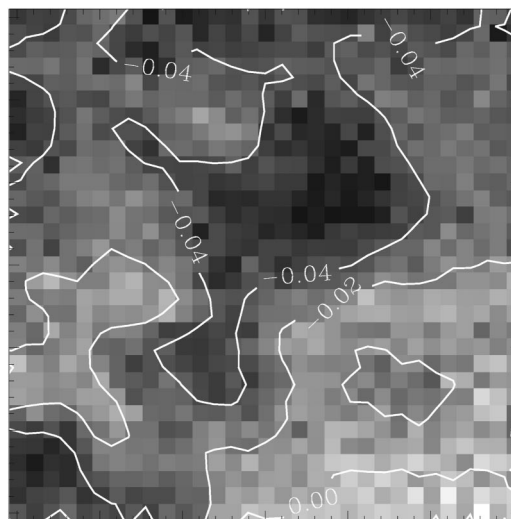


FIG. 4. Two-dimensional scan of a HoFe₂ crystal, measured with the circularly polarized microprobe. The brightness of each spot is proportional to the measured flipping ratio at this point. Clearly, domain structures can be identified.

quency on the order of 10^{-1} Hz during these scans. Figure 3 shows the measured flipping ratio as a function of energy.

After setting the beam energy to the found optimum at 8.075 keV (Ho L-III edge), the circularly polarized microprobe was used to image the magnetic domain structure of the HoFe₂ crystal. Preliminary magnetic force microscopy scans had determined regions with in-plane magnetic domains. Observing the (400) Bragg reflection of the crystal, two-dimensional scans of the regions of interest were performed while reversing the helicity of the incident beam to obtain the flipping ratio for each point on the sample. Figure 4 shows the measured flipping ratio for a $30 \mu\text{m} \times 30 \mu\text{m}$ area. Obviously, regions with different flipping ratios can be identified. According to Eq. (4), these differences in the measured signal can be attributed to changes in the direction of the local magnetic moment.¹²

In summary, a circularly polarized x-ray beam with high degree of polarization and small beam cross-section could be produced. The beam was polarized up to 99%. The beam spot had a size of about $4 \times 2 \mu\text{m}$. With this beam, a two-dimensional scan of a HoFe₂ crystal was performed while simultaneously switching the helicity of the polarization. Clearly, domain structures in the sample could be identified by the different flipping ratios of the illuminated areas. In the near future, the setup will be used to perform measurements on materials like spring magnets or magnetic multilayers. To improve the spatial resolution, the use of a microzone plate with smaller zone structure is planned. An electromagnet capable of delivering fields of up to 0.8 T is under commissioning.

ACKNOWLEDGMENTS

We would like to thank B. Lai and Z. Cai for providing the Fresnel zone plate used in these experiments. Research at the Advanced Photon Source is supported by U.S. DOE-BES under Contract No. W-31-109-ENG-38.

- ¹M. Blume and D. Gibbs, *Phys. Rev. B* **37**, 1779 (1988).
- ²K. Hirano, T. Ishikawa, and S. Kikuta, *Nucl. Instrum. Methods Phys. Res. A* **336**, 343 (1993).
- ³K. Hirano, K. Izumi, T. Ishikawa, S. Annaka, and S. Kikuta, *Jpn. J. Appl. Phys., Part 2* **30**, L407 (1991).
- ⁴J. C. Lang and G. Srajer, *Rev. Sci. Instrum.* **66**, 1540 (1995).
- ⁵C. Giles, C. Malgrange, J. Goulon, C. Vettier, F. de Bergevin, A. Freund, and P. Elleaume, *Proc. SPIE* **2010**, 136 (1993).
- ⁶*X-ray Microscopy and Spectromicroscopy*, edited by J. Thieme, G. Schmahl, D. Rudolph, and E. Umbact (Springer, Berlin, 1998).
- ⁷M. Born and E. Wolf, *Principles of Optics* (Cambridge University Press, Cambridge, 1980).
- ⁸G. Schmahl and P.-C. Cheng, in *Handbook on Synchrotron Radiation*, edited by S. Ebashi, M. Koch, and E. Rubenstein (Elsevier Science, New York, 1991).
- ⁹Q. Shen and K. D. Finkelstein, *Phys. Rev. B* **45**, 5075 (1992).
- ¹⁰K. Hirano, K. Kanzaki, M. Mikami, M. Miura, K. Tamasaku, T. Ishikawa, and S. Kikuta, *J. Appl. Crystallogr.* **25**, 531 (1992).
- ¹¹S. Pizzini, M. Bonfim, F. Baudalet, H. Tolentino, A. San Miguel, K. Mackay, C. Malgrange, M. Hagelstein, and A. Fontaine, *J. Synchrotron Radiat.* **5**, 1298 (1998).
- ¹²G. Srajer *et al.* (to be published).